International Journal of Thermophysics, Vol. 28, No. 1, February 2007 (© 2007)
DOI: 10.1007/s10765-007-0164-4

Isochoric Heat-Capacity Measurements for Pure Methanol in the Near-Critical and Supercritical Regions

N. G. Polikhronidi,[1] I. M. Abdulagatov,[2–4] G. V. Stepanov,[1] and R. G. Batyrova[1]

Received December 4, 2006

Isochoric heat-capacity measurements for pure methanol are presented as a function of temperature at fixed densities between 136 and 750 kg·m^{-3}. The measurements cover a range of temperatures from 300 to 556 K. The coverage includes the one- and two-phase regions, the coexistence curve, the near-critical, and the supercritical regions. A high-temperature, high-pressure, adiabatic, and nearly constant-volume calorimeter was used for the measurements. Uncertainties of the heat-capacity measurements are estimated to be 2–3% depending on the experimental density and temperature. Temperatures at saturation, $T_S(\rho)$, for each measured density (isochore) were measured using a quasi-static thermogram technique. The uncertainty of the phase-transition temperature measurements is 0.02 K. The critical temperature and the critical density for pure methanol were extracted from the saturated data (T_S, ρ_S) near the critical point. For one near-critical isochore (398.92 kg·m^{-3}), the measurements were performed in both cooling and heating regimes to estimate the effect of thermal decomposition (chemical reaction) on the heat capacity and phase-transition properties of methanol. The measured values of C_V and saturated densities (T_S, ρ_S) for methanol were compared with values calculated from various multiparametric equations of state (EOS) (IUPAC, Bender-type, polynomial-type, and nonanalytical-type), scaling-type (crossover) EOS, and various correlations. The measured C_V data have been analyzed and interpreted in terms of extended scaling equations for

[1]Institute of Physics of the Dagestan Scientific Center of the Russian Academy of Sciences, M. Yaragskogo Str. 94, 367005 Makhachkala, Dagestan, Russia.
[2]Present address: Physical and Chemical Properties Division, National Institute of Standards and Technology, 325 Broadway, Boulder, Colorado 80305, U.S.A.
[3]Institute for Geothermal Problems of the Dagestan Scientific Center of the Russian Academy of Sciences, Shamilya Str. 39, 367003 Makhachkala, Dagestan, Russia.
[4]To whom correspondence should be addressed. E-mail: ilmutdin@boulder.nist.gov

the selected thermodynamic paths (critical isochore and coexistence curve) to accurately calculate the values of the asymptotical critical amplitudes ($A_0^{\pm}$ and B_0).

KEY WORDS: adiabatic calorimeter; coexistence curve; critical amplitude; critical exponents; critical point; crossover equation of state; isochoric heat capacity; methanol; quasi-static thermograms.

1. INTRODUCTION

Pure fluids of species that hydrogen bond behave differently from systems that interact only through dispersion forces. For pure fluids, strong attractive interactions between like molecules result in the formation of molecular clusters that have considerable effect on the thermodynamic and structural properties of the species. The anomalous structural and thermodynamic properties of highly associated fluids are governed by hydrogen bonding. In contrast to physical interactions, chemical interactions (hydrogen-bonding) are short-ranged and highly directional. Presently, statistical mechanics (calculation of the structural and thermodynamic properties of a fluid from knowledge of the intermolecular interactions) can give inaccurate or even physically incorrect results when applied to hydrogen-bonded fluids. Due to its high polarity and strong self-association, methanol has a complex structure and is a challenge to study both experimentally and theoretically. We do not have a sufficient understanding of microscopic properties of associated fluids including the nature of hydrogen bonds and their effect on the thermodynamic properties. A deeper understanding of the structure and nature of hydrogen-bonding fluids and their effect on the thermodynamic behavior will lead to marked improvements in important practical applications in the environmental, mechanical, chemical, biological, and geothermal industries. Pure alcohols at high temperatures can be thermally unstable. Experiments that measure thermodynamic properties of a thermally labile species over a wide temperature range are often hindered by chemical reactions, including decomposition. A number of previous studies have studied the effects of methanol decomposition on the thermodynamic properties of methanol [1–6]. It has been reported that a serious complication exists at $T > 405\,\mathrm{K}$, since methanol begins to decompose at this temperature.

The design of engineering systems utilizing methanol requires an accurate knowledge of the thermodynamic properties. For example, it is well-known that the addition of a polar co-solvent (methanol, for example) to a supercritical fluid (H_2O or CO_2) often leads to an enhancement in the solubility of a solute and an improvement of the selectivity

of the supercritical solvent (effective polar modifiers) [7–11]. Methanol has been often used as an effective modifier for H_2O and CO_2 in supercritical fluid extraction and in supercritical chromatography. The use of methanol as a co-solvent can modify the polarity and solvent strength of the primary supercritical fluid to increase the solute solubility and selectivity and to minimize operating costs in an extraction process. A survey of the literature reveals that measurements of the thermodynamic properties of pure methanol in the near-critical and the supercritical regions are very scarce. The chief objective of this paper is to provide accurate isochoric heat-capacity data ($C_V VT$) and phase-boundary properties (T_S, ρ_S) for pure methanol in the near-critical and supercritical regions.

2. PREVIOUS ISOCHORIC HEAT-CAPACITY, SATURATED-DENSITY, AND CRITICAL-PARAMETER MEASUREMENTS FOR METHANOL

2.1. Isochoric Heat-capacity Measurements

Due to the thermal instability of methanol molecules, published thermodynamic data for methanol display significant scatter that is larger than the author's claimed uncertainties. Therefore, it is difficult to select experimentally consistent thermodynamic data sets that can be used to develop accurate equations of state (EOS) or correlations. This is one of the reasons why there are large differences between various EOS and correlation calculations for pure methanol. Experimental thermodynamic data of pure methanol were reviewed and compiled extensively under the auspices of IUPAC [12]. De Reuck and Craven [12] reported a comprehensive review of all of the methanol measurements which were made between 1887 and 1992. No isochoric heat-capacity data were published before 1992. The IUPAC [12] formulated EOS for pure methanol was developed without accurate $C_V VT$ data; therefore, this EOS cannot be used to accurately calculate the caloric properties of pure methanol, especially in the critical and supercritical regions where a scaling-type critical anomaly of thermodynamic properties is observed. Eubank [13] reported also, in 1970, a review of earlier work on the thermodynamic and other physical properties of methanol. In our recent papers (Abdulagatov et al. [14] and Aliev et al. [15]), we reviewed also new publications on thermodynamic properties of pure methanol, after 1992. Therefore, here we will briefly review only work where isochoric heat-capacity, phase-boundary, and critical-properties data were reported.

Recently, a limited number of measurements of the $C_V VT$ properties for pure methanol have been reported by various authors [4, 14–18]. The measurements of Aliev et al. [15], Kitajima et al. [16], and Kuroki

et al. [17] cover the low-temperature (below 420 K) range in the liquid phase. Abdulagatov et al. [4] reported $C_V VT$ data for methanol (purity of 99.3%, 0.5 mass% of H_2O) along six isochores in the density range from 266 to 449 $kg \cdot m^{-3}$ and at temperatures from 443 to 521 K. The uncertainty of the measured values of heat capacity in the critical region was 3%. After the measurements, gases thought to be decomposition products, were released from the calorimetric cell. The measurements are not high quality due to impurity effects on the near-critical behavior of isochoric heat-capacity and phase-transition properties (saturated densities and temperatures near the critical point). A shift in the saturation temperature for each measured density was found during cooling and heating passes, again due to decomposition reactions. Suleimanov [18] reported comprehensive measurements of the isochoric heat capacities of pure methanol in the temperature range from 470 to 620 K and at densities between 68 and 526 $kg \cdot m^{-3}$. These temperature and density ranges included one- and two-phase regions, coexistence curve, and near- and supercritical regions. Most measurements were performed near the phase-transition points to accurately extract the coexistence curve data (T_S, ρ_S) near the critical point. The uncertainty in heat-capacity measurements was 1.5–5.5% depending on the range of temperature and density. Recently, Abdulagatov et al. [14] reported isochoric heat-capacity measurements for pure methanol in the immediate vicinity of the critical point for densities between 274.87 and 331.59 $kg \cdot m^{-3}$ and at temperatures from 482 to 533 K including the coexistence curve. Measurements were performed along one vapor and five liquid isochores. The uncertainty of these data is 2–3%. These data were used to develop the crossover model for the thermodynamic properties of pure methanol. The present isochoric heat-capacity measurements considerably expand the temperature and density ranges in which C_V data for pure methanol are available.

2.2. Saturated-density Measurements

Very restricted experimental saturated-liquid and -vapor density data are available for pure methanol in the critical region [4, 6, 14, 18–29]. Suleimanov [18] reported near-critical saturated densities for pure methanol (water content of less than 0.04 mass% and an organic content less than 0.02 mass%) by observing the discontinuity in the ischoric heat capacity at the phase-transition boundary along each fixed isochore. Fifteen values of the saturated-liquid and -vapor densities were reported by Suleimanov [18] in the temperature range from 483.15 K to the critical temperature, 512.70 K. Values of the critical density ($\rho_C = 267.38\ kg \cdot m^{-3}$) and the critical temperature ($T_C = 512.70 \pm 0.2$ K on IPTS-68) were extracted from

the measured values of saturated density and temperature in the critical region.

Abdulagatov et al. [14] also used an isochoric-heat-capacity experiment together with the quasi-static thermograms technique (see Section 3.2) to measure saturated densities for pure methanol in the critical region. They reported six values of the saturated boundary properties (T_S, ρ_S'', ρ_S') for pure methanol in the critical region. The uncertainties of the phase-transition temperature and density measurements were, respectively, 0.02 K and 0.15%. Six values of the saturated density and saturated temperature were also obtained from the $C_V VT$ measurements by Abdulagatov et al. [4]. Bazaev et al. [6] used isothermal ($P-\rho$) and isochoric ($P-T$) break-point techniques to determine saturated densities for methanol in the temperature range from 423.15 to 503.15 K. Saturated-liquid and -vapor densities of pure methanol were reported by Efremov [20] in the temperature range from 273 to 513.15 K. Measurements were made by using a visual method. No uncertainties for the measured values of density are given in the work.

Cibulka [21] has critically evaluated all of the published experimental saturated-liquid densities for pure methanol. He reported the parameters of a correlating equation (non-scaling type equation) and recommended values of the saturated-liquid densities for pure methanol. The temperature range for the experimental saturated-density data was from 175.4 to 508.51 K. The relative RMSD of the correlation was 0.18% or 1.03 kg·m^{-3}. Unfortunately, this correlation does not include the critical region between 508.51 K and T_C. The relative differences between various correlations [12,21,23,24,27,29] in the critical region (from 490 to 512.6 K) reached a maximum of 2%. The same difference (about 2%) is found between the critical densities reported by various authors (see Section 2.3). Overall 43 experimental saturated-density data points were found in the literature in the temperature range from 505 K to T_C.

2.3. Critical Properties Data

Gude and Teja [30] and Abdulagatov et al. [14] have reviewed the critical property data of pure methanol. Gude and Teja [30] recommended critical properties data ($T_C = 512.5 \pm 0.2$ K, $\rho_C = 273 \pm 2$ kg·m^{-3}, $P_C = 8.084 \pm 0.02$ MPa) with their uncertainties. All of the available experimental and estimated critical-properties (temperature, pressure, and density) data for methanol lie in the range between 505.2 and 536.2 K, 7.065 and 9.701 MPa, and 267.4 and 358.7 kg·m^{-3}, respectively [30]. The scatter of reported values of the critical-temperature, the critical-pressure, and the critical-density data from the values recommended by Gude and Teja

[30] lie between −23.7 and 7.3 K, −1.62 and 1.02 MPa, and −85.7 and 4.0 kg·m^{-3}, respectively. This can be explained primarily by the effect of methanol decomposition on measured values of the critical parameters. Most reported values of the critical temperature of methanol after 1955 lie within 512.2–512.8 K, while before 1955 all reported data lay within 512.9 to 513.9 K. Newer methods (flow method; transient pulse-heating thin-wire probe) have been proposed by various authors to measure the critical parameters for thermally unstable fluids or reactive compounds. These newer methods are capable of residence times between 0.01 ms and 30 s. Unfortunately, these newer methods have not been applied to measurement of the critical parameters of methanol. These could be valuable, particularly if the typical measurement uncertainties can be reduced.

3. EXPERIMENTAL

3.1. Isochoric Heat-capacity Measurements

The isochoric heat capacities of pure methanol were measured with a high-temperature, high-pressure, adiabatic, and nearly constant-volume calorimeter with an uncertainty of 2–3% depending on the range of temperature and density. The theory and physical basis of the method of the heat-capacity measurements, and details of the apparatus, procedures, and uncertainty assessment have been described in our previous publications [31–41]; therefore, only essential information will be given here. In this method the heat capacities at constant volume are obtained by measuring the heat input necessary for a given temperature change of a fluid contained in a spherical calorimeter. The heat capacity is obtained from measurements of the following quantities: m, mass of the fluid in the calorimeter; ΔQ, electrical energy dissipated by the inner heater; ΔT, temperature change resulting from addition of an energy ΔQ; and C_0, empty calorimeter heat capacity as [31–41]

$$C_V = \frac{1}{m}\left(\frac{\Delta Q}{\Delta T} - C_0\right), \tag{1}$$

where the empty-calorimeter heat capacity (in J·K^{-1}) was calculated from the equation,

$$C_0 = 0.1244T - 1.037 \times 10^{-4}T^2 + 60.12 \tag{2}$$

and T is the temperature in K. The values of the empty-calorimeter heat capacity were determined as a function of temperature by using reference heat-capacity data for He^4 [42], which is well-known with an uncertainty

of 0.2%. The density of the sample at a given temperature T and pressure P is calculated from the simple relation,

$$\rho = m / V_{PT}, \tag{3}$$

where m is the filling mass of the sample in the calorimeter and $V_{PT} = \Delta V_T + \Delta V_P$ is the temperature- and pressure-dependent volume of the calorimeter. The temperature dependence of the calorimeter volume at fixed pressure was calculated as

$$\Delta V_T = V_{T_0} [1 + 3\alpha_T (T - T_0)], \tag{4}$$

where $V_{T_0} = 105.405 \pm 0.01\,\text{cm}^3$ is the volume of the calorimeter at a reference temperature $T_0 = 293.65\,\text{K}$ and at atmospheric pressure and α_T is the thermal expansion coefficient of the calorimeter material (stainless steel 10X18H9T) as a function of temperature,

$$\begin{aligned} \alpha_T = {} & 14.6 \times 10^{-6} + 1.59 \times 10^{-8} (T - 273.15) - 0.23 \times 10^{-10} \\ & \times (T - 273.15)^2 + 0.013 \times 10^{12} (T - 273.15)^3 \end{aligned} \tag{5}$$

where T is the temperature in K. The uncertainty in the α_T calculation is about 2%. The value of V_{T_0} was previously calibrated from the known density of a standard fluid (pure water) with well-known PVT values (IAPWS standard, Wagner and Pruß [43]). The pressure dependence of the calorimeter volume ΔV_P was calculated from the Love formula (Keyes and Smith [44]) for a thick-walled sphere. The uncertainty in the calorimeter volume V_{PT} at a given temperature and pressure is about 0.04%. The uncertainty of the mass m of the sample is estimated to be 0.006%. The total maximum experimental uncertainty in the density determination is 0.06%. The temperature was measured with a PRT-10 mounted in a tube inside the calorimetric sphere. The uncertainty of the temperature measurements was less than 15 mK. The thermometer was calibrated on ITS-90 by comparison with a standard thermometer of the VNIIFTRI (Moscow).

A detailed uncertainty analysis of the method (all of the measured quantities and corrections) is given in our previous publication [36]. The uncertainty in C_V due to departures from full adiabatic control is $0.013\,\text{kJ}\cdot\text{K}^{-1}$. The correction related to the deviation from true isochores during heating, $(C_V - C_V^{\text{exp}})$, was determined to an uncertainty of about 4.0–9.5% depending on the density. Based on a detailed analysis of all sources of uncertainties likely to affect the determination of C_V with the present system, the combined expanded ($k = 2$) uncertainty of measuring the heat-capacity, with allowance for the propagation of uncertainty

related to the departure from true isochoric conditions of the heating process, was 2–3% in the near-critical and supercritical regions, 1.0–1.5% in the liquid phase, and 3–4% in the vapor phase.

The heat-capacity is measured as a function of temperature at nearly constant density. The calorimeter was filled at room temperature, sealed, and heated along a quasi-isochore. Each run was normally started in the two-phase (L–V) region and completed in the one-phase (liquid or vapor depending on the filling density) region at its highest temperature or pressure. Between the initial (L–V) and the final single-phase state, the system undergoes a liquid–gas phase transition. This method enables one to determine with good accuracy the transition temperature T_S, the jump in the heat-capacity ΔC_V, and reliable C_V data in the one- and two-phase regions for each quasi-isochore (see Section 3.2).

For a selected near-critical isochore ($398.92\,kg{\cdot}m^{-3}$) after reaching the maximum measured temperature of 511 K, the sample was cooled to 493 K (initial temperature) and C_V was measured in order to compare with the results from a heating run. The presence of some gases, which were not identified, in the calorimeter after measurements were completed, has been observed. A residual pressure, due to presence of the gaseous phase after measurements in the calorimeter (the calorimeter was cooled with liquid nitrogen before opening), was noted. After completion of the measurements for a given isochore, the calorimeter was discharged, and a new sample was used to continue measurements for other isochores.

3.2. Phase-boundary Properties (T_S, ρ'_S, ρ''_S, C'_{V1}, C''_{V1}, C'_{V2}, and C''_{V2}) Measurements: Method of Quasi-static Thermograms

The one- (C'_{V1}, C''_{V1}) and two-phase (C'_{V2}, C''_{V2}) vapor and liquid heat capacities at saturation, the saturated temperature (T_S), and saturated-liquid (ρ'_S) and -vapor (ρ''_S) densities can also be measured by the method described above (see Section 3.1). The method of quasi-static thermograms (isochoric heat-capacity jumps and temperature versus time, $T-\tau$, plot) was used in this work to accurately determine the location of the phase-boundary parameters (T_S, ρ'_S, ρ''_S) of pure methanol. Details of the method of quasi-static thermograms and its application to complex thermodynamic systems with different types of phase transitions (pure fluids and binary solutions with L–V, L–L, L–S, V–S, L–S–V, and L–L–S phase-transitions) are described in recent publications [36,40,41,45–47].

The construction of the calorimeter described above enables control of the thermodynamic state of the measuring system with two independent sensors, namely, (a) a resistance thermometer-PRT ($T-\tau$ plot) and (b) a layer of cuprous oxide (Cu_2O) surrounding the calorimetric vessel

that serves as an adiabatic shield (integral adiabatic screen). In comparison with earlier work with the quasi-static thermogram technique by Chashkin et al. [48] and by Voronel [49], the present method of thermograms ($T-\tau$ plot) here is supplemented by recording readings of the sensor of adiabatic control. With synchronously recorded readings of the resistance thermometer and of the cuprous oxide sensor of adiabatic control, one can monitor the thermodynamic state of the fluid that approaches the phase-transition point (phase-transition temperature, T_S) at a fixed density (ρ'_S or ρ''_S). Precisely at the liquid–vapor phase-transition curve, the heat capacity is known to change discontinuously, leading to a sharp change in the thermogram slope ($dT/d\tau$). The high sensitivity of cuprous oxide makes it possible to determine exactly the temperature changes on a strip-chart recorder. Temperature changes are recorded on a thermogram tape of a pen recorder as a spike produced by the Cu_2O sensor and as a break (change of the thermogram slope). The coincidence in time of the positions of the spike in the Cu_2O sensor signal and of the break in the slope of the sample temperature thermogram indicates that the processes occurring in the system are quasi-static. Indeed, the Cu_2O responds to a change in the thermodynamic state of the sample at the internal surface of the calorimeter, while the resistance thermometer (PRT) records temperature changes in the center of the calorimeter. The presence of any temperature gradient in the volume of the sample would shift the positions of the spike and the break in the thermogram. However, with temperature changes occurring at rates of 5×10^{-5} to $10^{-4}\,\mathrm{K\cdot s^{-1}}$, the shift is observed to be less than $10^{-4}\,\mathrm{K}$. In regions with a weak temperature dependence of the heat capacity, the thermogram segments are virtually rectilinear and have a constant slope.

The method of continuous heating used to measure the heat-capacity allows one not only to accurately determine the phase-transition temperature, but also to directly measure, from the break in the thermogram, the magnitude of the heat-capacity jump ΔC_V from the break of slopes of the thermograms as

$$\Delta C_V = k\left[\left(\frac{d\tau}{dT}\right)_{VT_S-\varepsilon} - \left(\frac{d\tau}{dT}\right)_{VT_S+\varepsilon}\right], \tag{6}$$

where $(d\tau/dT)_{VT_S-\varepsilon}$ and $(d\tau/dT)_{VT_S+\varepsilon}$ are the slopes of the thermograms before and after the phase-transition temperature T_S, respectively; k is a coefficient depending on the magnitude of the heat flow and the mass of the sample; and T_S is the temperature of the phase transition corresponding to the fixed isochore. It is well-known (Sengers and Levelt Sengers [50, 51]) that the isochoric heat-capacity jump ΔC_V diverges at the

critical point as $\Delta C_V \propto (T - T_C)^{-\alpha}$, where $\alpha = 0.112$ is the universal critical exponent. Therefore, the difference, $\left[(d\tau/dT)_{VT_S-\varepsilon} - (d\tau/dT)_{VT_S+\varepsilon}\right]$, between thermogram slopes before $(d\tau/dT)_{VT_S-\varepsilon}$ and after $(d\tau/dT)_{VT_S+\varepsilon}$ a phase-transition in the critical region is very large (about 30–50% depending on the filling factor). This fact has allowed a very sensitive determination of phase transitions near a critical point. Conversely, the $P-T$ isochoric break-point or $P-\rho$ isothermal break-point techniques are much less sensitive to a phase transition in the critical region because the slopes of the $P-T$ and $P-\rho$ curves change very little due to the small difference between the densities of the phases in equilibrium. Therefore, the quasi-static thermogram method is more sensitive to determine phase-boundary properties than $P-T$ and $P-\rho$ break-point techniques in the critical region. At conditions far from the critical point, $P-T$ and $P-\rho$ break-point techniques are preferred because the heat-capacity jump ΔC_V is small (therefore, changes in thermogram slopes also are small), while the slopes of the $P-T$ isochores and the $P-\rho$ isotherms exhibit breaks that are sharp. Measurements of the temperatures and densities corresponding to the phase-transition curve using the method of quasi-static thermograms in the above-described adiabatic calorimeter are carried out as follows. The calorimeter is filled with the fluid to the target density; then, the apparatus is brought into the working range of temperatures, and is held until adiabatic conditions are established. After this, thermograms are recorded. In order to check the reproducibility (± 0.02 K) of the phase-transition temperature at fixed density, the measurements were made for both heating and cooling. When one isochore is completed, part of the sample is extracted from the calorimeter into a measuring vessel and the amount of the fluid extracted is measured. The measurements are then repeated at the new fixed density.

3.3. Test Measurements

To check and confirm the reliability and accuracy of the method and procedures for the C_V and phase-boundary property (T_S, ρ'_S, ρ''_S) measurements, measurements were first carried out for pure water and toluene at selected densities. Tables I and II provide the experimental C_V and (T_S, ρ'_S, ρ''_S) data for pure water and toluene measured using the same experimental apparatus together with values calculated from reference equation of state (IAPWS formulation, Wagner and Pruß [43] and Lemmon and Span [52]). Table I shows that the agreement between test measurements of C_V for pure water and toluene and reference EOS [43, 52] calculations is excellent (AAD = 1.13% and 0.81%, respectively). Table II shows that the differences between measured and calculated saturated

Table I. Validation Measurements of C_V on Pure Water and Toluene in the One- and Two-phase Regions

Water					
T(K)	C_V^{exp} (kJ·kg^{-1}·K^{-1})	C_V [43] (kJ·kg^{-1}·K^{-1})	T(K)	C_V^{exp} (kJ·kg^{-1}·K^{-1})	C_V [43] (kJ·kg^{-1}·K^{-1})
	$\rho = 971.82$ kg·m^{-3}			$\rho = 309.60$ kg·m^{-3}	
352.53	4.183	4.196	643.05	10.30	10.50
368.77	3.768	3.755	645.91	12.07	12.19
392.95	3.584	3.595	649.33	5.137	5.185
416.31	3.425	3.463	844.21	2.575	2.507
AAD (%)	0.50		AAD (%)	1.75	
Toluene					
T(K)	C_V^{exp} (kJ·kg^{-1}·K^{-1})	C_V [52] (kJ·kg^{-1}·K^{-1})	T(K)	C_V^{exp} (kJ·kg^{-1}·K^{-1})	C_V [52] (kJ·kg^{-1}·K^{-1})
	$\rho = 777.80$ kg·m^{-3}			$\rho = 555.25$ kg·m^{-3}	
392.825	1.581	1.561	545.840	2.049	2.029
393.604	1.563	1.563	548.720	2.034	2.035
399.339	1.621	1.582	549.315	2.054	2.036
411.334	1.614	1.622	550.413	2.046	2.039
AAD (%)	1.05		AAD (%)	0.56	

densities for pure water and toluene are within 0.05% and 0.15%, respectively, although for toluene in the critical region the difference increases to 1.7%. Table II also shows that the differences between measured and calculated phase-transition temperatures are good. For toluene the difference ranges from 0.9 K for a high density (777.8 kg·m^{-3}) to about 0.3 K for the near-critical densities, while for water it is less than 0.05 K. This good agreement for test measurements demonstrates the reliability and accuracy of the present method for C_V measurements.

4. RESULTS AND DISCUSSION

Measurements of the isochoric heat capacity for pure methanol were performed along nine liquid isochores (750.08, 714.24, 701.85, 689.56, 647.59, 592.10, 548.37, 499.75, and 398.92 kg·m^{-3}) and seven vapor isochores (265.77, 258.07, 244.33, 241.06, 212.16, 206.16, and 136.14 kg·m^{-3}). The temperature range was 300–556 K. The commercial supplier of the

Table II. Validation Measurements of Phase-boundary Properties (T_S, ρ_S) on Pure Water and Toluene

Water			
T_S (K)	ρ_S (kg·m^{-3})	ρ_S [43] (kg·m^{-3})	Difference (%)
572.480	45.620	45.658	−0.08
647.090	309.60	309.84	−0.08
647.104	321.96	–	–
353.070	971.82	971.82	0.00
ρ_S (kg·m^{-3})	T_S (K)	T_S [43] (K)	Difference (K)
45.620	572.430	572.430	0.05
309.60	647.090	647.090	0.00
321.96	647.104	–	–
971.82	353.060	353.060	0.01
Toluene			
T_S (K)	ρ_S (kg·m^{-3})	ρ_S [52] (kg·m^{-3})	Difference (%)
385.900	777.80	775.90	0.24
545.302	555.25	555.69	−0.08
589.544	214.64	218.27	−1.69
ρ_S (kg·m^{-3})	T_S (K)	T_S [52] (K)	Difference (K)
777.80	385.900	385.05	0.85
555.25	545.302	545.50	−0.20
214.64	589.544	589.26	0.28

methanol provided a purity analysis of 99.95 mol%. The experimental one- and two-phase C_V data and ($C_{V1}, C_{V2}, T_S, \rho_S$) values on the coexistence curve are given in Tables III and IV and shown in Figs. 1–6 as projections in the $C_V - T$ and $C_V - \rho$ planes, together with values reported by other researchers [17,18] and calculated with various EOS (crossover model [14], IUPAC [12], Bender-type [53], and Kozlov [27]). The densities presented in Table III (quasi-isochores) are the values of densities calculated from Eq. (3), where V_{PT} is the value of the calorimeter volume at the saturation temperature, T_S. The maximum deviation of the values of density from those at saturation is ±0.65%. The full range of experimental C_V as a function of temperature along the liquid, vapor, and near-critical isochores is shown in Fig. 1. Figure 2 shows the temperature dependence of the measured values of the isochoric heat capacity for pure methanol at four near-critical densities in both the one- and

Table III. Experimental Values of the One- and Two-phase Isochoric Heat Capacities of Methanol[a]

T (K)	C_V (kJ·kg^{-1}·K^{-1})	T (K)	C_V (kJ·kg^{-1}·K^{-1})	T (K)	C_V (kJ·kg^{-1}·K^{-1})	T (K)	C_V (kJ·kg^{-1}·K^{-1})
$\rho = 750.08$,kg·m^{-3}		$\rho = 714.24$,kg·m^{-3}		$\rho = 701.85$,kg·m^{-3}		$\rho = 689.56$,kg·m^{-3}	
300.062	2.750	313.078	2.761	325.290	2.780	332.247	2.836
300.446	2.753	313.322	2.755	325.648	2.775	332.612	2.841
300.693	2.744	313.560	2.758	325.010	2.783	332.843	2.839
309.603	2.739	313.810	2.763	349.746	2.991	333.082	2.850
309.854	2.756	331.170	2.770	349.813	2.975	333.320	2.833
309.227	2.760	331.779	2.749	349.999	2.980	349.514	2.996
311.012	2.697	332.010	2.753	371.813	3.145	349.980	2.984
311.385	2.744	339.488	2.889	371.965	3.148	350.442	2.990
311.870	2.769	339.509	2.893	372.140	3.156	351.710	3.003
325.419	2.775	339.891	2.874	372.560	3.140	352.063	2.998
325.650	2.748	340.613	2.880	374.340	3.159	352.052	3.012
325.011	2.771	341.122	2.879	374.893	3.144	362.672	3.084
325.130	2.739	341.966	2.887	375.112	3.173	363.001	3.070
332.960	2.794	354.130	2.974	376.890	3.187	363.477	3.092
333.200	2.780	354.470	2.990	377.220	3.166	373.667	3.170
333.680	2.837	354.700	2.953	377.843	3.164	374.011	3.175
334.272	2.817	368.981	3.122	377.919	3.178	374.568	3.178
334.633	2.806	369.205	3.117	378.101	3.187	375.781	3.182
334.980	2.822	369.430	3.119	378.980	3.161	376.220	3.190
335.112	2.840	370.190	3.141	379.536	3.180	376.658	3.179
335.580	2.842	370.301	3.141	379.860	3.188	390.459	3.272
335.934	2.847	370.524	3.129	380.417	3.191	390.567	3.274
336.171	2.845	370.859	3.149	380.855	3.174	390.831	3.280
336.526	2.834	370.970	3.140	381.188	3.199	391.108	3.284
336.880	2.852	**371.082**	**3.145**	381.383	3.205	391.324	3.288
337.117	2.855	**371.082**	**2.706**	381.821	3.197	391.540	3.292
337.188	**2.858**	371.193	2.695	382.040	3.201	391.757	3.296
337.188	**2.520**	371.528	2.699	**382.150**	**3.215**	391.865	3.298
337.235	2.537	371.863	2.725	**382.150**	**2.735**	**391.970**	**3.300**
337.353	2.519	372.309	2.700	382.588	2.729	**391.970**	**2.805**
337.944	2.524	372.532	2.733	382.917	2.733	392.082	2.800
338.417	2.513	373.847	2.725	383.575	2.740	392.406	2.802
340.062	2.542	374.110	2.700	383.684	2.742	392.622	2.808
340.300	2.539	374.560	2.719	385.670	2.769	392.838	2.793
340.538	2.550	378.320	2.725	385.890	2.783	393.055	2.810
340.881	2.533	378.540	2.734	386.220	2.810	393.271	2.814
343.264	2.555	378.716	2.739	386.553	2.794	393.488	2.792
343.319	2.549	381.733	2.750	390.242	2.819	397.570	2.890
343.425	2.549	381.820	2.763	390.570	2.847	397.792	2.863
346.386	2.563	381.919	2.758	390.906	2.830	398.216	2.884
346.644	2.567	392.619	2.822	403.177	2.884	403.868	2.915

Table III. Continued

T (K)	C_V (kJ·kg^{-1}·K^{-1})	T (K)	C_V (kJ·kg^{-1}·K^{-1})	T (K)	C_V (kJ·kg^{-1}·K^{-1})	T (K)	C_V (kJ·kg^{-1}·K^{-1})
347.080	2.558	392.824	2.837	403.341	2.894	404.083	2.890
352.409	2.583	392.917	2.835	403.619	2.917	404.412	2.903
352.867	2.587	392.992	2.840	403.805	2.919	405.993	2.915
–	–	–	–	–	–	406.625	2.925
$\rho = 647.59$ kg·m^{-3}		$\rho = 592.10$ kg·m^{-3}		$\rho = 548.37$ kg·m^{-3}		$\rho = 499.75$ kg·m^{-3}	
349.167	2.990	421.290	3.590	313.644	2.760	474.392	4.670
349.422	2.993	421.630	3.649	313.795	2.758	474.619	4.679
349.713	2.990	421.810	3.622	313.933	2.773	474.993	4.684
359.383	3.065	422.020	3.598	326.141	2.810	484.569	4.879
359.567	3.078	433.238	3.865	326.252	2.813	484.752	4.893
359.964	3.082	433.641	3.894	326.649	2.847	484.945	4.869
371.885	3.163	433.855	3.895	326.790	2.820	485.233	4.880
372.013	3.174	434.220	3.880	349.273	2.998	487.926	5.020
372.440	3.155	444.807	4.005	349.465	3.014	488.118	5.028
391.220	3.320	445.103	4.022	349.916	3.007	488.406	5.064
391.543	3.325	445.507	4.037	372.442	3.198	488.608	5.088
391.869	3.316	449.512	4.048	372.613	3.175	489.177	5.080
391.970	3.318	449.844	4.063	372.948	3.180	489.370	5.089
416.512	3.572	450.011	4.044	373.117	3.175	489.563	5.098
416.823	3.580	452.917	4.096	394.239	3.395	489.940	5.110
417.130	3.564	453.041	4.107	394.640	3.418	490.035	5.118
422.019	3.602	453.810	4.120	394.998	3.422	490.131	5.117
422.226	3.604	454.210	4.012	435.376	3.915	490.227	5.133
422.537	3.613	454.513	4.050	435.612	4.012	490.323	5.135
422.744	3.610	454.709	4.066	455.619	4.200	**490.418**	**5.140**
422.951	3.613	454.902	4.078	455.834	4.187	**490.418**	**3.620**
423.158	3.616	455.101	4.090	455.999	4.193	490.514	3.622
423.261	3.623	455.300	4.107	456.207	4.219	490.610	3.617
423.364	3.619	455.598	4.122	465.585	4.355	490.705	3.600
423.468	**3.620**	455.697	4.126	465.944	4.407	490.991	3.598
423.468	**2.935**	455.797	4.132	473.513	4.497	491.278	3.579
423.571	2.915	455.896	4.138	474.488	4.531	491.469	3.564
423.675	2.930	455.996	4.144	474.585	4.535	491.660	3.582
423.778	2.946	**456.095**	**4.150**	474.683	4.539	491.851	3.565
426.470	2.930	**456.095**	**3.170**	474.780	4.542	491.947	3.529
426.681	2.943	456.194	3.165	474.878	4.546	499.379	3.267
427.012	2.938	456.586	3.144	**474.975**	**4.550**	499.473	3.270
427.223	2.951	456.781	3.161	**474.975**	**3.325**	499.663	3.248
431.295	2.990	456.879	3.166	475.072	3.320	499.758	3.230
431.605	3.015	457.074	3.158	475.170	3.321	507.791	3.184
431.907	3.035	457.269	3.158	475.267	3.318	507.979	3.197
442.719	3.054	457.463	3.160	475.461	3.305	508.167	3.175
442.922	3.050	462.241	3.122	475.656	3.288	508.355	3.170
443.093	3.048	462.630	3.134	475.850	3.265	512.581	3.130

Table III. Continued

T (K)	C_V (kJ·kg^{-1}·K^{-1})	T (K)	C_V (kJ·kg^{-1}·K^{-1})	T (K)	C_V (kJ·kg^{-1}·K^{-1})	T (K)	C_V (kJ·kg^{-1}·K^{-1})
–	–	462.935	3.120	476.045	3.278	512.743	3.147
–	–	463.221	3.119	483.217	3.273	512.900	3.134
–	–	469.022	3.128	483.990	3.273	–	–
–	–	469.319	3.134	487.119	3.273	–	–
–	–	469.614	3.128	487.899	3.273	–	–
–	–	473.717	3.150	–	–	–	–
$\rho = 398.92$ kg·m^{-3}		$\rho = 265.77$ kg·m^{-3}		$\rho = 258.07$ kg·m^{-3}		$\rho = 244.33$ kg·m^{-3}	
493.669	5.822	494.909	6.837	474.976	5.920	494.146	7.054
493.814	5.830	495.195	6.849	475.170	5.937	494.336	7.088
493.971	5.833	495.481	6.875	475.365	5.957	494.527	7.139
503.169	6.360	503.212	7.511	475.559	5.964	494.718	7.128
503.374	6.377	503.447	7.549	486.004	6.484	501.162	7.645
503.641	6.390	503.719	7.584	486.643	6.459	501.370	7.713
503.917	6.401	503.922	7.619	486.824	6.472	501.944	7.754
505.530	6.522	507.603	8.017	496.908	7.124	507.038	8.134
505.726	6.538	507.791	8.153	497.099	7.160	507.226	8.167
505.910	6.544	507.979	8.203	497.384	7.155	507.415	8.277
506.195	6.527	508.168	8.151	497.575	7.078	507.603	8.350
506.477	6.642	512.046	9.803	503.074	7.655	510.412	9.470
506.764	6.670	512.234	10.364	503.357	7.620	510.790	9.559
507.042	6.681	512.422	10.586	503.640	7.718	511.071	9.639
507.221	6.693	512.515	10.830	503.735	7.620	511.352	9.745
507.415	6.705	512.609	11.135	508.638	8.450	511.726	9.998
507.509	6.722	512.702	11.673	508.826	8.489	512.007	10.260
507.697	6.764	**512.775**	**12.250**	509.108	8.364	512.289	10.637
507.791	6.756	**512.775**	**6.410**	509.296	8.567	512.382	10.791
508.073	6.770	512.796	6.369	510.987	9.360	512.440	11.158
508.262	6.807	512.890	6.254	511.268	9.439	512.534	11.360
508.356	6.833	512.983	6.098	511.455	9.525	512.628	11.599
508.450	6.820	513.077	5.980	511.602	9.635	**512.665**	**11.680**
508.525	**6.840**	513.186	5.887	511.830	9.748	**512.665**	**6.105**
508.525	**4.350**	513.288	5.797	512.112	10.061	512.721	6.022
508.540	4.348	513.375	5.710	512.206	10.205	512.815	5.897
508.641	4.290	516.602	5.077	512.377	10.550	512.908	5.781
508.733	4.245	516.788	4.861	512.470	10.798	513.068	5.590
508.931	4.178	516.882	4.729	512.564	11.100	513.189	5.516
509.110	4.169	517.068	4.740	512.657	11.613	513.376	5.380
509.313	4.137	517.162	4.677	512.751	11.972	513.657	5.246
509.394	4.151	522.571	4.432	**512.758**	**12.000**	513.938	5.122
509.672	4.110	522.760	4.396	**512.758**	**6.383**	514.314	5.000
509.954	4.099	522.949	4.388	512.845	6.239	516.415	4.729
510.236	4.043	523.233	4.393	512.938	6.055	516.602	4.673
510.518	4.022	–	–	513.032	5.951	516.788	4.719
510.706	4.013	–	–	513.062	5.918	516.975	4.620

Table III. Continued

T (K)	C_V (kJ·kg^{-1}·K^{-1})	T (K)	C_V (kJ·kg^{-1}·K^{-1})	T (K)	C_V (kJ·kg^{-1}·K^{-1})	T (K)	C_V (kJ·kg^{-1}·K^{-1})
–	–	–	–	513.264	5.630	522.560	4.396
–	–	–	–	513.548	5.390	522.745	4.401
–	–	–	–	513.736	5.288	522.931	4.389
–	–	–	–	514.017	5.183	523.117	4.355
–	–	–	–	514.485	5.039	531.988	4.063
–	–	–	–	516.975	4.723	532.172	4.070
–	–	–	–	517.068	4.697	532.448	4.040
–	–	–	–	517.255	4.670	532.724	4.049
–	–	–	–	517.441	4.709	–	–
–	–	–	–	523.209	4.139	–	–
–	–	–	–	523.395	4.186	–	–
–	–	–	–	523.673	4.119	–	–
–	–	–	–	523.859	4.138	–	–
$\rho = 241.06$ kg·m^{-3}		$\rho = 212.16$ kg·m^{-3}		$\rho = 206.16$ kg·m^{-3}		$\rho = 136.14$ kg·m^{-3}	
416.013	4.022	478.278	6.573	486.004	7.163	482.149	8.533
416.342	4.050	478.643	6.588	486.349	7.172	482.643	8.580
416.610	4.037	478.864	6.595	486.617	7.204	482.912	8.941
416.917	4.013	494.527	7.609	491.645	7.612	487.926	9.177
435.477	4.654	494.718	7.647	491.758	7.643	488.149	9.203
435.783	4.637	494.909	7.654	491.916	7.670	488.622	9.248
435.908	4.670	495.099	7.690	492.144	7.698	488.863	9.266
436.209	4.688	505.246	8.751	503.735	8.520	491.758	9.574
455.243	5.345	505.532	8.758	504.019	8.593	492.076	9.648
455.617	5.369	505.723	8.730	504.208	8.698	492.313	9.719
455.899	5.370	505.976	8.733	504.491	8.729	492.540	9.660
456.312	5.366	510.336	10.022	510.330	9.840	494.146	9.820
475.172	6.070	510.523	10.080	510.517	9.943	494.336	9.913
475.364	6.111	510.898	10.223	510.799	10.378	494.803	9.744
475.512	6.095	511.273	10.499	511.080	10.432	503.168	10.826
475.749	6.122	511.461	10.607	511.269	10.596	503.451	10.837
475.997	6.119	511.554	10.660	511.455	10.700	503.735	10.829
494.077	7.173	511.648	10.746	511.549	10.787	503.829	10.844
494.349	7.155	511.742	10.845	511.643	10.951	504.266	10.863
494.668	7.210	511.836	10.960	511.737	11.100	504.361	10.890
504.003	7.899	511.930	11.085	**511.772**	**11.135**	504.450	10.886
504.267	7.944	**512.005**	**11.210**	**511.772**	**5.350**	**504.531**	**10.890**
504.379	7.919	**512.005**	**5.450**	511.830	5.319	**504.531**	**5.220**
504.719	7.934	512.020	5.443	511.924	5.249	504.549	5.137
511.081	9.655	512.114	5.387	512.206	5.094	504.644	4.688
511.362	9.848	512.207	5.322	512.394	5.030	504.738	4.573
511.643	10.050	512.394	5.238	512.582	4.976	504.832	4.502
511.831	10.182	512.488	5.199	512.770	4.927	504.907	4.495
512.018	10.352	512.675	5.120	513.052	4.845	507.306	4.462

Table III. Continued

T (K)	C_V (kJ·kg^{-1}·K^{-1})	T (K)	C_V (kJ·kg^{-1}·K^{-1})	T (K)	C_V (kJ·kg^{-1}·K^{-1})	T (K)	C_V (kJ·kg^{-1}·K^{-1})
512.112	10.410	513.050	5.007	513.334	4.781	507.494	4.465
512.206	10.688	513.331	4.922	513.616	4.730	507.682	4.458
512.394	11.045	513.613	4.860	514.086	4.666	508.261	4.456
512.487	11.224	514.083	4.768	514.277	4.643	513.236	4.215
512.580	11.540	516.975	4.460	521.910	4.155	513.517	4.167
512.633	**11.605**	517.162	4.484	522.188	4.139	513.798	4.163
512.633	**6.000**	517.441	4.467	522.374	4.142	522.467	3.885
512.674	5.960	517.535	4.450	522.652	4.113	522.652	3.864
512.768	5.864	519.585	4.365	–	–	522.838	3.850
512.862	5.719	519.771	4.370	–	–	523.024	3.861
512.956	5.690	519.957	4.339	–	–	531.712	3.720
513.236	5.463	520.238	4.330	–	–	531.896	3.733
513.517	5.288	532.080	3.910	–	–	532.172	3.719
513.798	5.125	532.361	3.895	–	–	532.357	3.726
514.088	5.010	532.547	3.905	–	–	–	–
514.455	4.928	532.733	3.890	–	–	–	–
519.119	4.590	543.435	3.820	–	–	–	–
519.306	4.575	543.709	3.820	–	–	–	–
519.585	4.490	544.074	3.819	–	–	–	–
519.678	4.496	544.438	3.819	–	–	–	–
525.342	4.140	544.712	3.837	–	–	–	–
525.619	4.125	545.076	3.837	–	–	–	–
525.834	4.147	545.350	3.817	–	–	–	–
526.040	4.154	545.623	3.822	–	–	–	–
537.142	4.020	555.671	3.753	–	–	–	–
537.319	4.037	555.852	3.753	–	–	–	–
537.589	4.017	556.212	3.754	–	–	–	–
537.992	4.025	–	–	–	–	–	–

[a] Values of density at saturated temperature and values of C_V at saturation curve are in bold.

two-phase regions together with values calculated with crossover (CREOS [14]) and multiparametric (IUPAC [12]) equations of state. This figure also includes the measurements reported by Suleimanov [18] at nearly the same densities. Figures 3 and 4 show the measured isochoric heat capacities of methanol along various liquid and vapor isochores (136.14, 212.16, 548.37, 592.10, 647.59, and 701.85 kg · m^{-3}) together with values calculated with the IUPAC [12] and Polt et al. [53] EOS and the data reported by Kuroki et al. [17] at a density of 705.5 kg·m^{-3}. The density dependence of the measured C_V along near- and supercritical isotherms together with values calculated with a crossover model [14] and the IUPAC [12]

Table IV. Experimental Isochoric Heat Capacities and Densities of Methanol at Saturation

T_S (K)	ρ'_S (kg·m^{-3})	C'_{V2} (kJ·kg^{-1}·K^{-1})	C'_{V1} (kJ·kg^{-1}·K^{-1})
337.188	750.08	2.858	2.520
371.082	714.24	3.145	2.706
382.150	701.85	3.215	2.735
391.970	689.56	3.300	2.805
423.468	647.59	3.620	2.935
456.095	592.10	4.150	3.170
474.975	548.37	4.550	3.325
490.418	499.75	5.140	3.620
508.525	398.92	6.840	4.350
T_S (K)	ρ''_S (kg·m^{-3})	C''_{V2} (kJ·kg^{-1}·K^{-1})	C''_{V1} (kJ·kg^{-1}·K^{-1})
512.775	265.77	12.250	6.410
512.758	258.07	12.000	6.383
512.665	244.33	11.680	6.105
512.633	241.06	11.605	6.000
512.005	212.16	11.210	5.450
511.772	206.16	11.135	5.350
504.531	136.14	10.890	5.220

EOS is presented in Fig. 5. The experimental values of liquid and vapor one-phase (C'_{V1}, C''_{V1}) and two-phase (C'_{V2}, C''_{V2}) isochoric heat capacities on the coexistence curve are shown in Fig. 6 together with values calculated with the IUPAC [12] and crossover [14] EOS. Figure 7 shows the measured vapor–liquid coexistence curve ($T_S - \rho_S$) data for pure methanol which were determined from the present C_V experiments by using the method of quasi-static thermograms in the critical region together with published data and values calculated from the crossover model by Abdulagatov et al. [14], multiparametric EOS [12,23,27,53], and correlations [21,24,29].

In order to study the effect of thermal decomposition of methanol molecules on measured values of phase-transition temperatures and isochoric heat capacities, the measurements for one selected isochore (398.92 kg·m^{-3}) were performed for both heating and cooling. As the measurements show, the maximum difference in C_V between both heating and cooling runs was about 0.5%, while the difference in T_S was within 0.25 K.

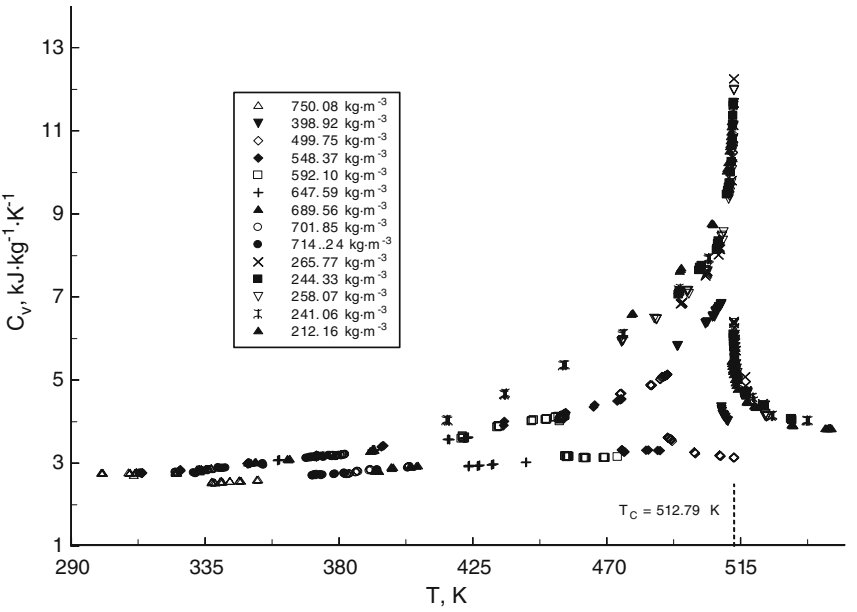

Fig. 1. Experimental isochoric heat capacities of methanol as a function of temperature along various liquid and vapor isochores near the critical point.

4.1. Comparisons with Published Data and Calculations with EOS

The measured C_V data for pure methanol were compared with values calculated from crossover models developed by Abdulagatov et al. [14] and multiparametric IUPAC [12] EOS. Figure 2 shows the experimental behavior of C_V as a function of temperature for methanol along the various near-critical isochores together with values calculated from a crossover model in the one- and two-phase regions. Good agreement (within 2.5%) was found for each near-critical isochore in the one-phase region at temperatures 1–3 K above the phase-transition point, while in the immediate vicinity of the phase-transition points the deviations reached as high as 14%. This is still acceptable because the present data have not been used to fit the parameters of the crossover model. Table V presents the AAD between the present measurements and the values calculated with the IUPAC [12] EOS for each measured density. As one can see from this table, the C_V deviations at liquid densities (750.08, 714.24, 701.85, 689.56, 499.75, and 398.92 $kg \cdot m^{-3}$) are within 5–7%, while at lower densities (647.59, 592.10, 548.37, and 212.16 $kg \cdot m^{-3}$) the agreement between measured and calculated values of C_V is excellent (AAD within 0.5–1.9%).

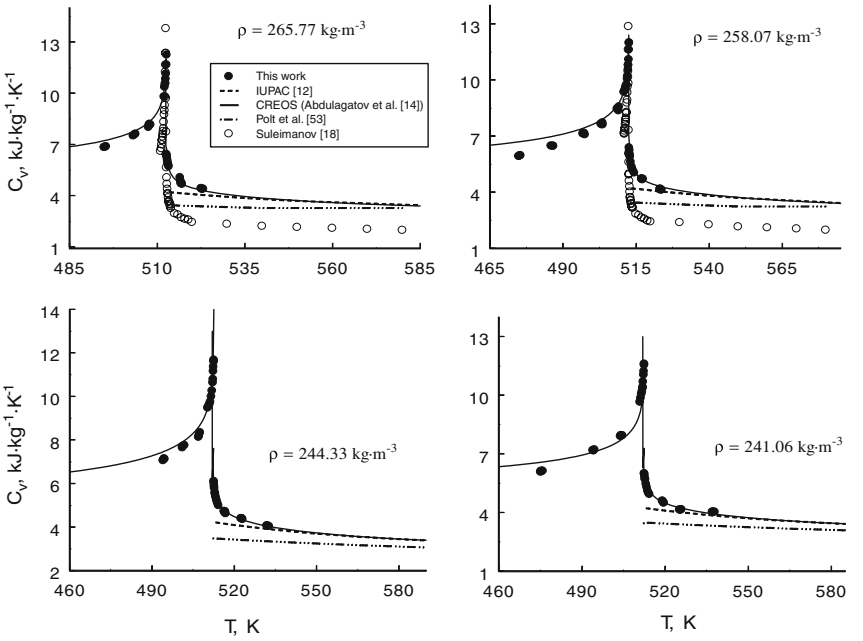

Fig. 2. Experimental isochoric heat capacities of methanol as a function of temperature along selected near-critical isochores together with values calculated from crossover model by Abdulagatov et al. [14], and IUPAC [12] and Polt et al. [53] EOS.

Good agreement (within 3.0%) was found for vapor isochores at 136.14 and 206.16 kg·m^{-3}. Almost all measured values of C_V were seen to be systematically higher than calculated values. In the critical and supercritical regions the discrepancy between measured and calculated values (IUPAC [12]) is as large as 30%. Good agreement, AAD = 2.9%, was observed for the one-phase saturated-liquid heat capacity C'_{V1} in the regular behavior region at temperatures up to about 7 K below the critical temperature. The discrepancy between measured and calculated saturated vapor heat capacities C''_{V1} is up to 30%, with calculated values systematically lower than measured values.

Figure 7 shows a comparison of the present saturated-density data and data reported by other authors and values calculated with various correlations in the critical region. A comparison of saturated-liquid densities reported in this work for methanol and values calculated with various correlations [21, 24, 29] and EOS [12, 23, 27, 53] is given in Table VI. Generally, all reported data and calculated values of saturated liquid densities agree within 0.4%, except for values calculated with the correlation by Zubarev and

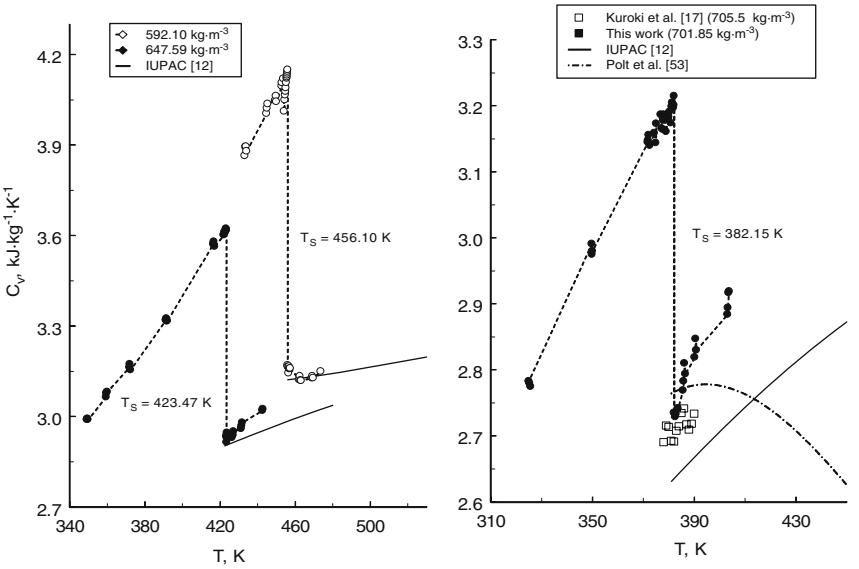

Fig. 3. Experimental one- and two-phase isochoric heat capacities of methanol as a function of temperature along liquid isochores near the phase-transition points together with values calculated from IUPAC [12] and Polt et al. [53] EOS and the data reported by Kuroki et al. [17].

Bagdonas [24]. Good agreement (within 0.2%) is found between the present measurements and values calculated with the Polt et al. [53] EOS and the correlation by Machado and Streett [22], while the values calculated from correlations by Cibulka [21], Kozlov [27], Goodwin [23], and Hales and Ellender [29] agree with the present results within 0.3%. The values of liquid density calculated with the correlation of Zubarev and Bagdonas [24] agree with the present results within 0.7%. The differences between the present saturated-vapor data and values calculated with the IUPAC [12] correlation are within 4.1%. The agreement between the present saturated-vapor densities and values calculated with the Goodwin [23] EOS is within 3.5%. The data by Donham [25] differ from the present saturated-vapor densities within 3.3%. Good agreement within 1.44% is found between the present saturated-vapor densities and the data reported by Straty et al. [28]. The deviations between the present data and the values reported by Suleimanov [18] for saturated densities in the critical region are within 2.8%. The data of Ramsey and Young [19] and Efremov [20] systematically differ by an even larger amount, almost up to 10% in the critical region. The saturated-density

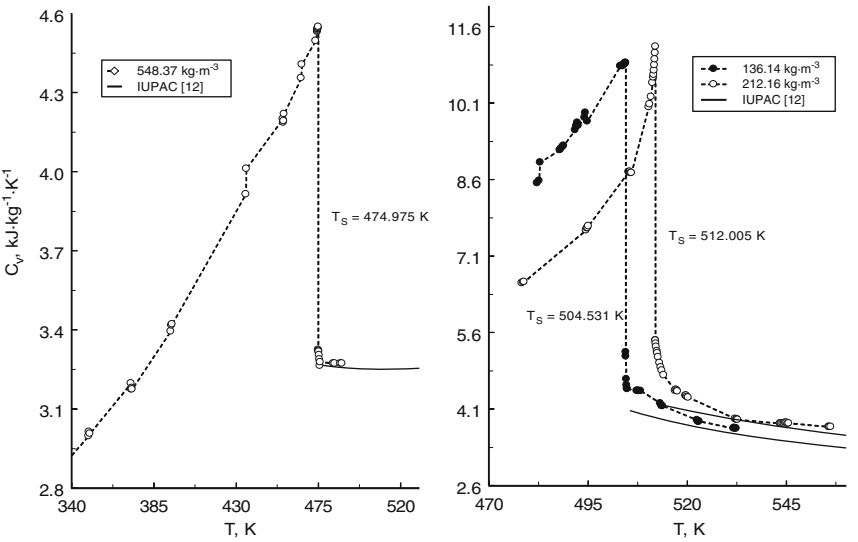

Fig. 4. Experimental one- and two-phase isochoric heat capacities of methanol as a function of temperature along liquid and vapor isochores near the phase-transition points together with values calculated from IUPAC [12] EOS.

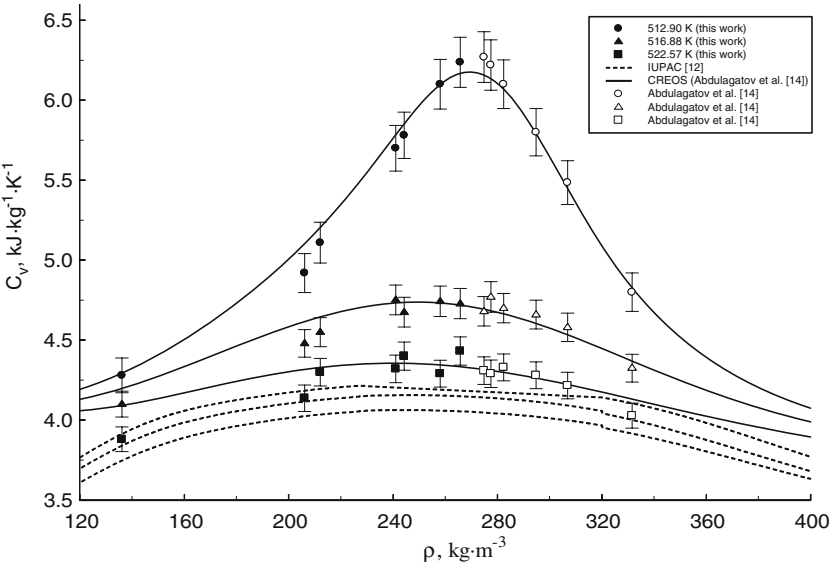

Fig. 5. Experimental one-phase isochoric heat capacities of methanol as a function of density along the near-critical and supercritical isochores together with values calculated with crossover model [14] and IUPAC [12] EOS.

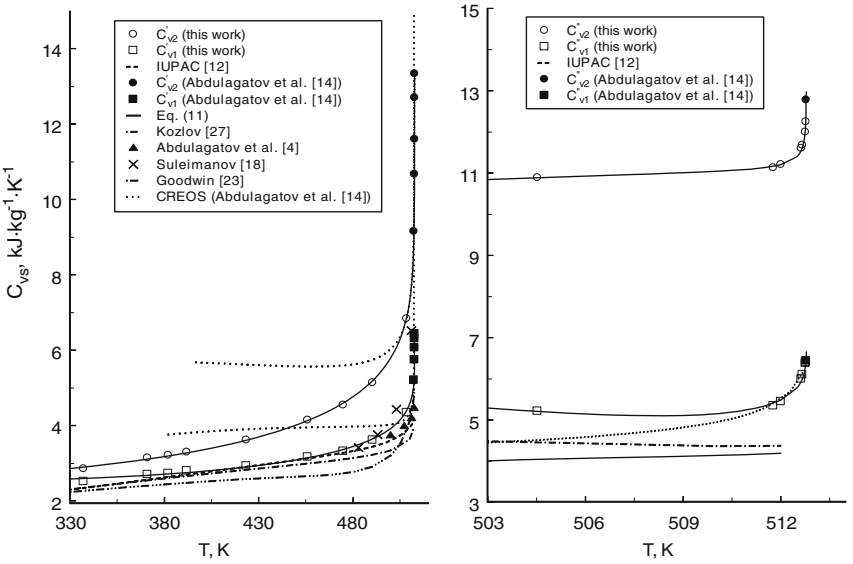

Fig. 6. Experimental liquid and vapor one-phase (C'_{V1}, C''_{V1}) and two-phase (C'_{V2}, C''_{V2}) isochoric heat capacities on the coexistence curve as a function of temperature near the critical point together with values calculated with scaling relations, Eqs. (10) and (11), and IUPAC [12] EOS.

data in the critical region reported by Bazaev et al. [6] show good agreement (AAD between 0.06% and 0.5%) with the present data.

4.2. Asymptotic and Nonasymptotic Scaling Behavior of the Isochoric Heat Capacity and Saturated Density of Methanol near the Critical Point

The theory of critical phenomena suggests that thermodynamic properties of fluids near the critical point exhibit the same singular asymptotic critical behavior as that of a lattice gas [54]. The theory of critical phenomena predicts that the asymptotic thermodynamic behavior of fluids near the critical point can be described in terms of the critical power laws and critical scaling laws [49, 55, 56] given by

$$\bar{C}_V = A_0^{\pm} t^{-\alpha}, \quad (\Delta\rho = 0, \text{ the critical isochore}), \tag{7}$$

$$\Delta\rho = B_0 t^{\beta}, \quad (\Delta\rho = \Delta\rho_{cxc}, \text{ coexistence curve}), \tag{8}$$

Table V. AAD between the Present C_V Measurements and Calculations from the IUPAC [12] EOS for Various Liquid and Vapor Isochores for Pure Methanol

ρ (kg·m^{-3})	AAD (%)
750.08	7.4
714.24	5.7
701.85	5.4
689.56	4.8
647.59	1.9
592.10	0.5
548.37	1.2
499.75	5.1
398.92	5.8
136.14	3.1
206.16	2.7
212.16	1.5

where $\bar{C}_V = C_V T_C / V P_C$, $\alpha = 0.112$, and $\beta = 0.325$ are the universal critical exponents [50, 51]; $\Delta\rho = (\rho - \rho_C)/\rho_C$; $t = (T_C - T)/T_C$; and $A_0^{\pm}$ and B_0 are the system-dependent critical amplitudes. According to scaling theory, the critical amplitude ratio (A_0^-/A_0^+) is universal [50, 51, 54, 57, 58];

$$\frac{A_0^-}{A_0^+} = [(1-2\beta)/(\gamma-1)]^2 (b^2-1)^{\alpha}, \tag{9}$$

where $b^2 = (\gamma - 2\beta)/\gamma(1-2\beta)$ is the universal constant. The theoretical value for this universal relationship is as follows: Ising model $A_0^+/A_0^- = 0.523$ [59]; field theory $A_0^+/A_0^- = 0.541$ [60]; ε-expansion $A_0^+/A_0^- = 0.520$ [60], and $A_0^+/A_0^- = 0.527$ from Eq. (9).

The range of validity of the asymptotical critical power laws, Eqs. (7) and (8), is restricted to a very small range of temperatures ($t < 10^{-2}$) and densities ($\Delta\rho < 0.25$) near the critical point. For comparison with a real experiment, it is very important to allow for the non-asymptotic corrections to the power laws, Eqs. (7) and (8), in the range where more reliable data can be obtained. In the asymptotic region, it is very difficult to obtain reliable experimental data because of the effects of gravity and other experimental difficulties. The allowance for Wegner's [61–64] corrections makes it possible to describe the non-asymptotic behavior of C_V and other thermodynamic functions along the critical isochore and coexistence

Table VI. Comparisons of the Present Saturated-liquid Densities with Values Calculated from Various EOS and Correlations for Pure Methanol

T_S (K)	ρ_S (kg·m^{-3}) (This work)	ρ_S (kg·m^{-3}) (IUPAC [12])	ρ_S (kg·m^{-3}) (Polt et al. [53])	ρ_S (kg·m^{-3}) (Cibulka [21])	ρ_S (kg·m^{-3}) (Machado [22])
337.188	750.08	748.80	749.00	748.69	748.63
371.082	714.24	713.27	713.10	713.07	712.92
382.150	701.85	700.60	700.35	700.45	700.33
391.970	689.56	688.76	688.51	688.69	688.63
423.468	647.59	645.72	646.02	646.09	646.69
456.095	592.10	588.36	590.59	589.07	589.62
474.975	548.37	544.42	548.45	544.92	–
490.418	499.75	495.83	502.19	496.61	–
508.525	398.92	391.66	399.35	396.27	–
AAD, %	–	0.38	0.20	0.33	0.21
T_S (K)	ρ_S (kg·m^{-3}) (Zubarev [24])	ρ_S (kg·m^{-3}) (Kozlov [27])	ρ_S (kg·m^{-3}) (Goodwin [23])	ρ_S (kg·m^{-3}) (Efremov [20])	ρ_S (kg·m^{-3}) (Hales [29])
337.188	748.46	748.92	748.25	751.46	748.72
371.082	712.25	712.75	712.73	716.22	713.13
382.150	698.81	699.90	699.97	703.02	700.51
391.970	686.60	687.98	688.12	691.21	688.75
423.468	642.56	645.24	645.34	643.00	646.13
456.095	585.23	589.17	588.89	592.84	589.30
474.975	541.29	545.47	545.68	546.30	545.62
490.418	493.30	497.63	497.96	499.97	498.27
508.525	390.64	397.78	390.72	401.43	401.28
AAD, %	0.73	0.33	0.33	0.31	0.27

curve and saturation density $\Delta\rho$ in the form,

$$\frac{C_V T_C}{V P_C} = \frac{A_0^+}{\alpha} t^{-\alpha}\left[1 + A_1^+ t^{\Delta} + A_2^+ t^{2\Delta} + \cdots\right] - B_{cr} \text{ for } \rho = \rho_C, T \geqslant T_C, \quad (10)$$

$$\frac{C_V T_C}{V P_C} = \frac{A_0^-}{\alpha} t^{-\alpha}\left[1 + A_1^- t^{\Delta} + A_2^- t^{2\Delta} + \cdots\right]. \text{ for } \rho = \rho_C \text{ at } T \leqslant T_C, \quad (11)$$

$$\Delta\rho = B_0 t^{-\alpha}(1 + B_1 t^{\Delta} + B_2 t^{2\Delta} + \cdots) \quad \text{for } T \leqslant T_C, \quad (12)$$

where $A_0^{\pm}$ and B_0 are the asymptotic critical amplitudes, $A_i^{\pm}$ and B_i ($i = 1, 2, \ldots$) are the critical amplitudes of the correction (nonasymptotic) terms of the Wegner's expansion, and $\Delta = 0.51$ is the universal critical exponent [65,66]. The numerical solution of the Ising lattice [63,64] also gives a similar series with a similar value for Δ.

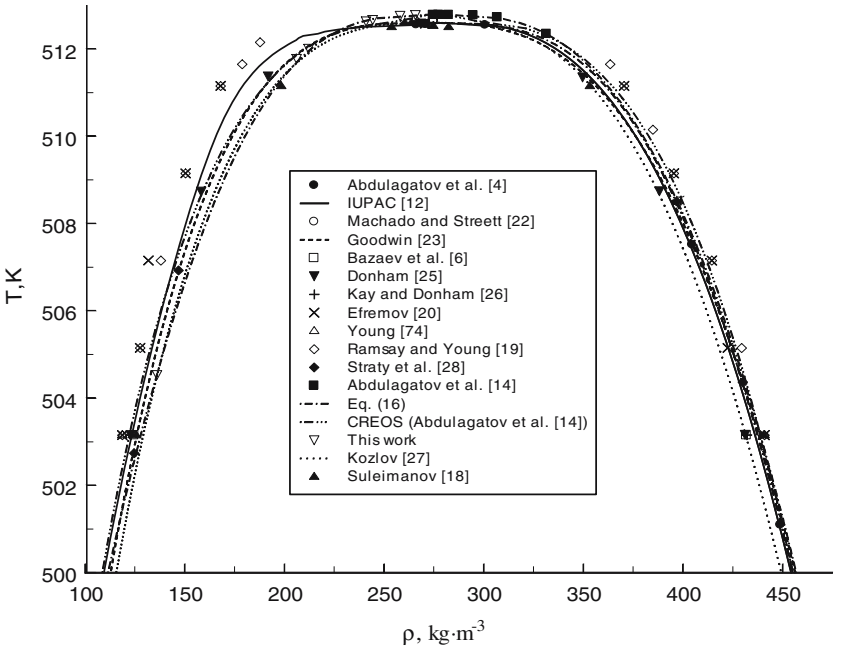

Fig. 7. Experimental liquid and vapor densities at saturation for pure methanol from the present C_V measurements together with reported values calculated from crossover model [14] and various correlations in the critical region.

Because the isothermal compressibility of the fluid is infinite ($K_T \to +\infty$) at the critical point, it is difficult to accurately measure the critical density directly. The mean of the densities of the saturated vapor (ρ_V) and saturated liquid (ρ_L), $\rho_d = (\rho_L + \rho_V)/2$ is a linear function of temperature,

$$\rho_d = B_1 + B_3 t. \tag{13}$$

The locus of the mean values ρ_d is known as the "rectilinear diameter". If this line is extrapolated to the critical temperature ($t \to 0$), the value obtained is the critical density ($\rho_d = \rho_C = B_1$). But more accurate measurements of the saturated densities showed that the rectilinear diameter ρ_d has a slight curvature ($\approx t^{1-\alpha}$, where $\alpha = 0.112$). According to the theory of liquid–gas critical phenomena based on renormalization group theory [67], the first temperature derivative ($d\rho_d/dT$) of the coexistence-curve diameter diverges as the isochoric heat capacity $t^{-\alpha}$ [68–71]. That is, as the reduced temperature t goes to zero ($t \to 0$), the diameter varies as

$$\Delta\rho_d \approx B_2 t^{1-\alpha} + B_3 t + \cdots, \tag{14}$$

where $\alpha = 0.112$ is the critical exponent that describes asymptotic behavior of the isochoric heat capacity (see Eq. (7)); B_3 is the amplitude of the rectilinear diameter of the coexistence curve. The rectilinear diameter exhibits a slight curvature in the immediate vicinity of the critical point. The data exhibit significant deviations from straight lines in the temperature range for which $t < 4 \times 10^{-2}$. Therefore, the value of the critical density determined from the singular-diameter law is less than that obtained from the linear extrapolation. The resulting uncertainty in the determination of the critical density is about 3–5%.

The effect of a Yang-Yang anomaly of strength R_μ on the coexistence-curve diameter is given by [72,73]

$$\Delta\rho_{\mathrm{d}} = b_{\mathrm{j}2} t^{2\beta} + a l_1 t^{1-\alpha} + c_1 t + \cdots \tag{15}$$

where $b_{\mathrm{j}2} = A_\mu / A_{\mathrm{P}}$, and A_μ, A_{P} are the critical amplitudes of second temperature derivatives of the vapor–pressure curve, $(d^2 P/dT^2)$ and the chemical potential, $(d^2\mu/dT^2)$, respectively. A Yang-Yang anomaly ($d^2\mu/dT^2 \to \pm\infty$) implies a leading correction $\Delta\rho_{\mathrm{d}} \approx t^{2\beta}$ would dominate the previously expected $\Delta\rho_{\mathrm{d}} \approx a l_1 t^{1-\alpha}$ correction [72,73]. But experimental resolution of the three corrections in Eq. (15) is very difficult.

The scaling expression for density along the coexistence curve in the critical region is

$$\Delta\rho = \pm B_0 t^{\beta} \pm B_1 t^{\beta+\Delta} + B_2 t^{1-\alpha} - B_3 t, \tag{16}$$

where

$$B_0 = k \Big/ (b^2-1)^{\beta},\ B_1 = kc \Big/ 2a(b^2-1)^{\beta+\Delta}$$

$$B_2 = \left[kb^4 \Big/ a(b^2-1)^{1-\alpha} \right] \left\{ \left[(e-\beta-2) \Big/ (5-2e) \right] (de_1 + f e_2) - \left[d(e-\beta) + f \right] \Big/ 3b^2 \right\},$$

B_0 is the asymptotic critical amplitude (Eq. 8); B_1 is the nonasymptotic critical amplitude (Wegner's correction term, Eq. (12)); B_2 is the singular diameter amplitude (Eq. (14)); B_3 is the rectilinear diameter amplitude (Eq. (13)); a, c, k are the parameters of the crossover equation of state; and, e, e_1, e_2, b^2 are the universal parameters determined from the universal critical exponents (α, β, Δ) [14]. Equations (10), (11), and (16) were applied to the present experimental C_{V} and saturated-density $(T_{\mathrm{S}}, \rho_{\mathrm{S}})$ data for methanol. The results are presented in Table VII and shown in Figs. 6 and 7. For methanol, the asymptotic critical amplitudes are $A_0^+ = 2.8601$

Table VII. Coefficients A_i and B_i for Eqs. (10), (11), and (16) ($T_C = 512.79\,K$; $P_C = 8.13\,MPa$; $V_C = 0.0036135\,m^3 \cdot kg^{-1}$; $\alpha = 0.112$; $\beta = 0.324$; $\Delta = 0.51$)

A_0	A_1	A_2	B_{cr}	Thermodynamic path
1.4797	−6.3144	3.7937	−3.7794	One phase along the coexistence curve C'_{V1} (liquid)
5.5268	−2.6797	1.4425	−3.1184	Two phase along the coexistence curve C'_{V2} (liquid)
0.5937	−44.6702	232.0708	−5.6933	One phase along the coexistence curve C''_{V1} (vapor)
2.7242	5.4561	−18.7822	−7.8213	Two phase along the coexistence curve C''_{V2} (vapor)
2.8601	3.8987	−20.8366	−1.8602	One phase along the critical isochore C_{V1} ($T > T_C$)
5.5004	−2.0927	−0.9806	−4.3286	Two phase along the critical isochore C_{V2} ($T < T_C$)
B_0	B_1	B_2	B_3	Thermodynamic path
1.8595	1.3372	4.0263	5.0141	Along the coexistence curve

and $A_0^- = 5.5004$, and $B_0 = 1.8595$, of the power laws for the isochoric heat capacity and the coexistence curve, respectively. As one can see, the value of the critical amplitude ratio (A_0^+/A_0^-) derived from the present C_V data is 0.52, which is in excellent agreement with values predicted by the Ising model [59], ε-expansion [60], and from a scaling EOS (Eq. (9)).

The fitting procedure was used to calculate the values of the critical parameters (T_C and ρ_C) for methanol. The critical temperature T_C and the critical density ρ_C in Eq. (16) were considered as adjustable parameters together with the critical amplitudes B_0, B_1, B_2, and B_3. The optimal values of the derived critical parameters are $T_C = 512.79 \pm 0.2\,K$ and $\rho_C = 276.74 \pm 2\,kg \cdot m^{-3}$. The present results for the critical temperature and the critical density deviate from the recommended values [30] by +0.29 K and $+3.74\,kg \cdot m^{-3}$ (1.4%), respectively.

5. CONCLUSIONS

The isochoric heat capacity for pure methanol was measured in the temperature range from 300 to 556 K, along nine liquid isochores (750.08, 714.24, 701.85, 689.56, 647.59, 592.10, 548.37, 499.75, and $398.92\,kg \cdot m^{-3}$) and seven vapor isochores (265.77, 258.07, 244.33, 241.06, 212.16, 206.16, and $136.14\,kg \cdot m^{-3}$), with a high-temperature and high-pressure adiabatic calorimeter. The results of the isochoric-heat-capacity and saturated-density measurements were compared with values calculated with crossover models and other multiparametric EOS. The liquid and vapor one-phase isochoric heat capacities, temperatures, and saturation densities were measured by using the quasi-static thermograms technique. A small effect (within 0.5%) of thermal decomposition of methanol on the measured val-

ues of the isochoric heat capacity is observed at high temperatures (above 453 K), while the effect of decomposition on the phase-transition temperature is significant (within 0.25 K for the near-critical isochores). The critical parameters (critical temperature and critical density) were derived from C_V measurements using the quasi-static thermograms technique for the phase-transition curve near the critical point. The measured results were used to analyze the critical behavior of the isochoric heat capacity of pure methanol in terms of the scaling theory of critical phenomena. The asymptotic critical amplitudes of A_0^+, A_0^-, and B_0 of the scaling laws were calculated from the measured values of C_V and saturated densities. The experimentally derived values of the critical amplitude ratio for C_V (A_0^+/A_0^-) are in good agreement with values predicted by scaling theory.

ACKNOWLEDGMENTS

One of us (I.M.A.) thanks the Physical and Chemical Properties Division at the National Institute of Standards and Technology for the opportunity to work at NIST during the course of this research. This work was also supported by the Grant of RFBR 05-08-18229-a and IAPWS International Collaboration Project Award.

REFERENCES

1. T. K. Yerlett and C. J. Wormald, *J. Chem. Thermodyn.* **18**:719 (1986).
2. G. C. Straty and A. M. F. Palavra, and T. J. Bruno, *Int. J. Thermophys.* **7**:1077 (1986).
3. R. Ta'ani, *Dr. Ing. Thesis* (Karlsruhe, 1976).
4. I. M. Abdulagatov, V. I. Dvorynchikov, M. M. Aliev, and A. N. Kamalov, in *Steam, Water, and Hydrothermal Systems, Proc. 13th Int. Conf. Prop. Water and Steam,* P. R. Tremaine, P. G. Hill, D. E. Irish, and P. V. Balakrishnan, eds. (NRC Research Press, Ottawa, 2000), pp.157–164.
5. T. J. Bruno and G. C. Straty, *J. Res. NBS* **91**:135 (1986).
6. A. R. Bazaev, I. M. Abdulagatov, J. W. Magee, and E. A. Bazaev, *J. Supercrit. Fluids* (in press).
7. S. S. T. Ting, S. J. Macnaughton, D. L. Tomasko, and N. R. Foster, *Ind. Eng. Chem. Res.* **32**:1471 (1993).
8. G. S. Gurdial, S. J. Macnaughton, D. L. Tomasko, and N. R. Foster, *Ind. Eng. Chem. Res.* **32**:1488 (1993).
9. J. M. Dobbs, J. M. Wong, R. J. Lahiere, and K. P. Johnston, *Ind. Eng. Chem. Res.* **26**:56 (1987).
10. M. P. Ekart, K. L. Bennett, S. M. Ekart, G. S. Gurdial, C. L. Liotta, and C. A. Eckert, *AIChE J.* **39**:235 (1993).
11. K. M. Dooley, Ch. -P. Kao, R. P. Gambrell, and F. C. Knopf, *Ind. Eng. Chem. Res.* **26**:2058 (1987).
12. K. M. De Reuck and R. J. B. Craven, *Methanol. International Thermodynamic Tables of the Fluid State-12* (Blackwell, Oxford, 1993).

13. P. T. Eubank,*Chem. Eng. Symp. Ser.* **66**:16 (1970).
14. I. M. Abdulagatov, S. B. Kiselev, J. F. Ely, N. G. Polikhronidi, and A. Abdurashidova, *Int. J. Thermophys.* **26**:1327 (2005).
15. M. M. Aliev, J. W. Magee, and I. M. Abdulagatov, *Int. J. Thermophys.* **24**:1527 (2003).
16. H. Kitajima, N. Kagawa, H. Endo, S. Tsuruno, and J. W. Magee, *J. Chem. Eng. Data* **48**:1583 (2003).
17. T. Kuroki, N. Kagawa, H. Endo, S. Tsuruno, and J. W. Magee, *J. Chem. Eng. Data* **46**:1101 (2001).
18. Ya. M. Suleimanov, Ph.D. Thesis (Power Eng. Research Inst., Baku, 1971).
19. W. Ramsay and S. Young, *Phyl. Trans. Roy. Soc.* (*London*) *A* **178**:313 (1887).
20. Yu. V. Efremov, *Russ. J. Phys. Chem.* **40**:1240 (1966).
21. I. Cibulka, *Fluid Phase Equilib.* **89**:1 (1993).
22. J. R. S. Machado and W. B. Streett, *J. Chem. Eng. Data* **28**:218 (1983).
23. R. D. Goodwin, *J. Phys. Chem. Ref. Data* **16**:799 (1987).
24. V. N. Zubarev and A. V. Bagdonas, *Teploenergetika* **4**:79 (1967).
25. W. E. Donham, Ph.D. Thesis (Ohio State University, Columbus, Ohio, 1953).
26. W. B. Kay and W. E. Donham, *Chem. Eng. Sci.* **4**:1 (1955).
27. A. D. Kozlov, *Methanol: Equations for Calculation of Thermophysical Properties*, private communication (Russian Research Center for Standardization, Information and Certification of Materials, Moscow, Russia, 2002).
28. G. C. Straty, M. J. Ball, and T. J. Bruno, *J. Chem. Eng. Data* **33**:115 (1988).
29. J. L. Hales and J. H. Ellender, *J. Chem. Thermodyn.* **8**:1177 (1976).
30. M. Gude and A. S. Teja, *J. Chem. Eng. Data* **40**:1025 (1995).
31. Kh. I. Amirkhanov, G. V. Stepanov, and B. G. Alibekov, *Isochoric Heat Capacity of Water and Steam* (Amerind Pub. Co., New Delhi, 1974).
32. N. G. Polikhronidi, I. M. Abdulagatov, J. W. Magee, and G. V. Stepanov, *Int. J. Thermophys.* **22**:189 (2001).
33. N. G. Polikhronidi, I. M. Abdulagatov, J. W. Magee, and G. V. Stepanov, *Int. J. Thermophys.* **23**:745 (2002).
34. N. G. Polikhronidi, I. M. Abdulagatov, J. W. Magee, and G. V. Stepanov, *Int. J. Thermophys.* **24**:405 (2003).
35. N. G. Polikhronidi, R. G. Batyrova, and I. M. Abdulagatov, *Int. J. Thermophys.* **21**:1073 (2000).
36. B. A. Mursalov, I. M. Abdulagatov, V. I. Dvoryanchikov, and S. B. Kiselev, *Int. J. Thermophys.* **20**:1497 (1999).
37. N. G. Polikhronidi, R. G. Batyrova, I. M. Abdulagatov, J. W. Magee, and G. V. Stepanov, *J. Supercrit. Fluids* **33**:209 (2004).
38. N. G. Polikhronidi, I. M. Abdulagatov, J. W. Magee, and R. G. Batyrova, *J. Chem. Eng. Data* **46**:1064 (2001).
39. I. M. Abdulagatov, N. G. Polikhronidi, and R. G. Batyrova, *J. Chem. Thermodyn.* **26**:1031 (1994).
40. N. G. Polikhronidi, R. G. Batyrova, and I. M. Abdulagatov, *Fluid Phase Equilib.* **175**:153 (2000).
41. N. G. Polikhronidi, I. M. Abdulagatov, and R. G. Batyrova, *Fluid Phase Equilib*. **201**:269 (2002).
42. N. B. Vargaftik, *Handbook of Physical Properties of Liquids and Gases*, 2nd edn. (Hemisphere, New York, 1983).
43. W. Wagner and A. Pruß, *J. Phys. Chem. Ref. Data* **31**:387 (2002).
44. F. G. Keyes and L. B. Smith, *Proc. Amer. Acad. Arts Sci.* **68**:505 (1933).

45. I. K. Kamilov, G. V. Stepanov, I. M. Abdulagatov, A. R. Rasulov, and E. I. Milikhina, *J. Chem. Eng. Data* **46**:1556 (2001).
46. I. M. Abdulagatov, B. A. Mursalov, and V. I. Dvoryanchikov, *J. Chem. Eng. Data* **45**:1133 (2000).
47. V. M. Valyashko, I. M. Abdulagatov, and J. H. M. Levelt-Sengers, *J. Chem. Eng. Data* **45**:1139 (2000).
48. Ya. R. Chashkin, V. A. Smirnov, and A. V. Voronel, *Thermophysical Properties of Substances and Materials*, (Moscow, GSSSD, 1970), Vol. 2, p. 139.
49. A. V. Voronel, in *Phase Transitions and Critical Phenomena*, C. Domb and M. S. Green, eds. (Academic Press, London, 1974), Vol. 5, p. 343.
50. J. V. Sengers and J. M. H. Levelt Sengers, *Progress in Liquid Physics*, C.A. Croxton, ed. (Wiley, New York, 1978).
51. J. V. Sengers and J. M. H. Levelt Sengers, *Ann. Rev. Phys. Chem.* **37**:189 (1986).
52. E. W. Lemmon and R. Span, *J. Chem. Eng. Data* **51**:785 (2006).
53. A. Polt , B. Platzer, and G. Maurer, *Chem. Tech. (Leipzig)* **44**:216 (1992).
54. M. E. Fisher, in *Critical Phenomena, Lectures Notes in Physics*, F. J. W. Hahne, ed. (Springer, Berlin, 1988), Vol. 186, p. 1
55. M. A. Anisimov and J. V. Sengers, in *Equations of State for Fluids and Fluid Mixtures*, J. V. Sengers, R. F. Kayser, C. J. Peters, and H. J. White Jr., eds. (Elsevier, Amsterdam, 2000).
56. S. C. Greer and M. R. Moldover, *Ann. Rev. Phys. Chem.* **32**:233 (1981).
57. M. A. Anisimov, *Critical Phenomena in Liquids and Liquid Crystals* (Gordon and Breach, Philadelphia, 1991).
58. M. Levy, J. C. Le Guillou, and J. Zinn-Justin, eds., *Phase Transitions*, Cargese 1980 (Plenum, New York, 1982).
59. A. J. Liu and M. E. Fisher, *Physica A* **156**:35 (1989).
60. C. Bagnuls, C. Bervilliev, D. I. Meiron, and B. C. Nickel, *Phys. Rev. B* **35**:3585 (1987).
61. F. J. Wegner, *Phys. Rev. B* **5**:4529 (1972).
62. M. Ley -Koo and M. S. Green, *Phys. Rev. A* **23**:2650 (1981).
63. D. M. Saul, M. Wortis, and D. Jasnow, *Phys. Rev. B* **11**:2571 (1975).
64. W. J. Camp and J. P. Van Dyke, *Phys. Rev. B* **11**:2579 (1975).
65. M. E. Fisher, S. -Y. Zinn, and P. J. Upton, *Phys. Rev.* **B59**:14533 (1999).
66. R. Guida and J. Zinn-Justin, *J. Phys. A Math Gen.* **31**:8103 (1998).
67. J. F. Nicoll, *Phys. Rev. A* **24**:2203 (1981).
68. F. Hensel, *Adv. Phys.* **44**:3 (1995).
69. N. D. Mermin, *Phys. Rev. Lett.* **26**:169 (1971).
70. J. J. Rehr and N. D. Mermin, *Phys. Rev. A* **8**:472 (1973).
71. B. Widom and J. S. Rowlinson,*J. Chem. Phys.* **52**:1670 (1970).
72. M. E. Fisher and G. Orkoulas, *Phys. Rev. Lett.* **85**:696 (2000).
73. G. Orkoulas, M. E. Fisher, and C. Ustün, *J. Chem. Phys.* **113**:7530 (2000).
74. S. Young, *Sci. Proc. Roy. Dublin Soc.* **21**:374 (1910).